Supplement

1 Mathematical Model

The transport rate v of a substrate x mediated by a transporter is in general described by Michaelis-Menten kinetics (Stein, 1990), i.e. $v = v_{max}\frac{x}{K_m+x}$. Since the substrate concentrations in our experiments are smaller, respectively in the order of the Michaelis-Menten constants of OATP1B3 and ABCC2 (Letschert et al., 2004; Cui et al., 2001), we linearized the Michaelis-Menten equation resulting in $v \approx \frac{v_{max}}{K_m}x =: px$. Thus, the translation of the model depicted in Fig. 2 into ordinary differential equations yields:

$$\begin{aligned}
\frac{dx_1(t)}{dt} &= -p_1x_1(t) - p_3x_1(t) + p_4x_3(t) - p_6x_1(t)(p_8 - x_2(t)) && (1)\\
&\quad +p_7x_2(t) - p_{12}\left(\frac{x_1(t)}{V_{bl}} - \frac{x_5(t)}{V_{ap}}\right)\\
\frac{dx_2(t)}{dt} &= p_6x_1(t)(p_8 - x_2(t)) - p_7x_2(t) && (2)\\
\frac{dx_3(t)}{dt} &= p_1x_1(t) - p_2x_3(t) + p_3x_1(t) - p_4x_3(t) && (3)\\
&\quad -p_5x_3(t) - p_9x_3(t)(p_{11} - x_4(t)) + p_{10}x_4(t)\\
\frac{dx_4(t)}{dt} &= p_9x_3(t)(p_{11} - x_4(t)) - p_{10}x_4(t) && (4)\\
\frac{dx_5(t)}{dt} &= p_2x_3(t) + p_5x_3(t) + p_{12}\left(\frac{x_1(t)}{V_{bl}} - \frac{x_5(t)}{V_{ap}}\right) && (5)
\end{aligned}$$

Here, x_1 is the amount of BSP unbound in the basolateral chamber, x_2 is BSP bound unspecifically to the filter membrane, x_3 is unbound intracellular BSP, x_4 is intracellular BSP bound to intracellular proteins, and x_5 is the amount of BSP in the apical chamber. The rate constants for OATP1B3 and ABCC2 are p_1 and p_2 respectively; p_3, p_4, and p_5 are the rate constants of the endogenous basolateral uptake transporter $Endo_{in-bl}$, the

endogenous basolateral efflux pump $Endo_{ex-bl}$, and the endogenous apical efflux pump $Endo_{ex-ap}$, respectively. The parameters p_6 and p_7 are the association and dissociation constants for unspecific binding to the filter membrane, the total capacity of which is denoted by p_8. The association and dissociation constants for the unspecific binding to intracellular proteins are p_9 and p_{10} respectively, whereas p_{11} denotes the total amount of intracellular binding proteins. The diffusion parameter of the paracellular transport is represented by p_{12}. V_{bl} and V_{ap} are the volumes of the basolateral and apical chamber, respectively.

It is not possible to observe all five components separately. Only the total intracellular content, $x_3 + x_4$, and the apical amount x_5 can be determined. For the preloading experiments, the basolateral amount x_1 was also determined. Thus, the observation equations for a given set of parameters $\vec{p} = (p_1, p_2, \ldots, p_{12})$ read:

$$\begin{aligned} y_1(t,\vec{p}) &= x_3(t,\vec{p}) + x_4(t,\vec{p}) \\ y_2(t,\vec{p}) &= x_5(t,\vec{p}) \\ y_3(t,\vec{p}) &= x_1(t,\vec{p}) \end{aligned}$$

1.1 Reduction of Parameter Space

Experiments showed that $86 \pm 1\%$ of the intracellular BSP is bound to intracellular proteins, independent of the total intracellular content of BSP under our conditions. Thus, for the steady state, the proportion of bound intracellular BSP to total intracellular BSP, $x_4/(x_3+x_4)$, has to be equal to 0.86.

Solving the steady state of Eqn. 4 for $x_4/(x_3 + x_4)$ yields:

$$\frac{x_4}{x_3 + x_4} = \left(\frac{p_{10}}{p_9} \frac{1}{p_{11} - x_4} + 1 \right)^{-1} \equiv 86\%$$

Since, as stated above, this identity is independent of the total intracellular content of BSP, the inequality $p_{11} \gg x_4$ has to hold. Thus, we get:

$$\begin{aligned} \frac{p_{10}}{p_9} &= \left(\frac{1}{0.86} - 1 \right) (p_{11} - x_4) \simeq \frac{0.14}{0.86} p_{11} \\ \Rightarrow p_{10} &= \frac{0.14}{0.86} p_{11} p_9 \end{aligned}$$

With $p_{11} \gg x_4$ and setting $k = p_9 p_{11}$, the model Eqs. 3 and 4 can be rewritten:

$$\begin{aligned}
\frac{dx_3}{dt} &= p_1 x_1 - p_2 x_3 + p_3 x_1 - p_4 x_3 \\
&\quad -p_5 x_3 - k x_3 + \frac{0.14}{0.86} k x_4 \\
\frac{dx_4}{dt} &= k x_3 - \frac{0.14}{0.86} k x_4,
\end{aligned}$$

leading to a reduction of the number of parameters from 12 to 10.

2 Penalized Likelihood Estimator

As described in *Methods*, experiments have been accomplished with the following experimental setups: Experiments with a concentration of BSP in the basolateral chamber of 10 nM and 10 μM, as well as preloading experiments. Each of these experiments was performed for control MDCKII cells, cells expressing OATP1B3, and cells expressing OATP1B3 and ABCC2 (Figs. 3-5). To describe all data sets with the model (Fig. 2), the parameters of the model had to be fitted to the data simultaneously by a multi-experiment analysis. The advantage of such an analysis is that non-identifiabilities of parameters can be resolved. For example, when the model was fitted solely to the data of an experiment with cells expressing OATP1B3, the amount of BSP transported either by OATP1B3 or by the endogenous transporter $Endo_{in-bl}$ could not be distinguished. Thus, only the sum of the parameters p_1 and p_3 could be determined, but not their individual values.

Since in the experiments performed with control cells there is only one basolateral uptake process, it is possible to determine the parameter p_3 in these experiments. By multi-experiment analysis, this knowledge about the value of p_3 from the control experiments is used to eliminate the non-identifiabilities in the other experiments.

2.1 Global and Local Parameters

In multi-experiment analysis, one has to distinguish between global and local parameters. Global parameters are those that have the same value for each experiment, whereas local parameters can differ from one experiment to another. Global parameters are parameters

such as chemical rate constants. In our model, the parameters p_6, p_7, p_9, and p_{10} are rate constants and are thus set to global parameters. Also, the total number of binding sites at the filter membrane, p_8, as well as the total number of intracellular binding sites, p_{11}, were assumed to be the same for all experiments and were thus treated as global parameters.

The amount and localization of the transport proteins varies depending on the time in culture, the induction of transporter expression and additional variance in the biological system. Thus, parameters that depend on protein concentrations, such as v_{max} values, can attain different values in different experiments. In our model, parameters $p_1 - p_5$ are proportional to the number of transporters per cell and were treated as local parameters.

Inulin experiments measuring the paracellular leakage also showed fluctuations in the amount of transported BSP. Therefore, we treated the diffusion parameter p_{12} as a local parameter as well.

The drawback of setting parameters to local ones is that for these parameters the advantages of the multi-experiment fit are lost. By definition, local parameters can vary independently and thus do not use the information provided by the other experiments. Again, this can lead to non-identifiabilities of parameters.

To resolve this issue, we introduced constrained local parameters (i.e., local parameters whose variations are bound to a predefined region around the mean of this parameter) over all experiments. We add constraints on the local parameters by introducing a penalized likelihood (Good and Gaskins, 1971).

2.2 Penalized Likelihood

To impose constraints on the variability of local parameters, we added a penalty term to the likelihood function that was to be maximized. In terms of Bayesian statistics, this penalty term contains prior knowledge of the distribution of the local parameters. Assuming Gaussian distributed local parameters, this penalty term reads:

$$\rho(p_{jl}) = \frac{1}{\sqrt{2\pi}\sigma_l} \exp\left(-\frac{(p_{jl} - \bar{p}_l)^2}{2\sigma_l^2}\right),$$

where p_{jl} is the value of local parameter l in experiment j, and $\bar{p}_l$ is the mean over all experiments. The standard deviation σ_l determines the size of the interval around the

mean value $\bar{p}_l$ that is accessible to the local parameters. For very large values of σ_l, (i.e., $\sigma_l \to \infty$), the penalty term is zero, and the local parameters p_l undergo no constraints. On the other hand, for $\sigma_l \to 0$, the smallest deviation of a local parameter p_{jl} from the mean value $\bar{p}_l$ leads to an infinite value of the penalty term, forcing all local parameters p_{jl} to attain the same value $\bar{p}_l$ (i.e., setting these local parameters to a global parameter).

If 66% of the local parameters p_{jl} are forced to be within an interval around the mean value $\bar{p}_l$, where the upper border of the interval is n_l-times the lower border, we get $\sigma_l = \frac{n_l-1}{n_l+1}\bar{p}_l$. For our model, we chose $n_l = 3$ for OATP1B3 and ABCC2, and $n_l = 1.5$ for the endogenous transporters as well as for the paracellular transport.

Let σ_{ijk} be the weight of the observed data, and y_{ijk} and $y_k(t_{ij})$ be the estimated value at time t_{ij} given the parameters $\vec{p}$. Then the penalized log-likelihood reads:

$$\mathcal{L}(p) = \sum_{i,j,k} \frac{\left(y_{ijk} - y_k(t_{ij}, p)\right)^2}{\sigma_{ijk}^2} + \sum_{j,l} \frac{\left(p_{jl} - \bar{p}_l\right)^2}{\left(\frac{n_l-1}{n_l+1}\bar{p}_l\right)^2}$$

Here, the first term is the usual least-square functional, with the sum running over data points i, all experiments j, and observables k. The second term is the logarithm of the penalty term with the sum running over all local parameters l and all experiments j.

3 Error Model

As described in *Methods*, the estimated mean values and standard deviations of the experiment presented in Figs. 3-5 were determined by triplicate measurements. Triplicate measurements were performed to give an estimate about the confidence interval of the estimated mean value. These confidence intervals are also subject to statistical fluctuations and thus cannot be determined with certainty. For Gaussian distributed random numbers, the 95% confidence interval of the estimated variances is (Honerkamp, 1994):

$$\sigma^2 \pm 1.96\sqrt{\frac{2}{N-1}}\sigma^2$$

For triplicate measurements (i.e., for $N = 3$), these intervals are very large, resulting in strong fluctuations in the estimated standard deviations (Supplement Fig. 8).

The plot of the estimated standard deviations versus the estimated mean values suggests a linear dependency (see Supplem Fig. 8). Using this linear relationship, we can re-estimate the standard deviations by a linear fit for each experiment. Thus, not only the three replicate measurements are used for to estimate standard deviation, but all measurements of one experiment. This leads to more reliable estimates of the standard deviations.

4 Model Selection

To justify the inclusion of the additional transport processes into our model, we compare the fit of the complete model with the fits of smaller models. Hereby, the smaller models are lacking either one of the endogenous transporters Endo$_{in-bl}$, Endo$_{ex-bl}$ and Endo$_{ex-ap}$, as well as the paracellular transport. Supplement Fig. 9 shows the resulting fits of the smaller models in comparison with the complete model. Hereby, for simplicity only the components with the most significant deviation of the fit of the smaller models from the experimental data are displayed.

Also, the Akaike Information Criterion (AIC) (Akaike, 1973) supports the choice of the complete model as the best model, see Supplement Table 2.

5 Fitting Results

The cumulative distributions of the local parameters resulting from the optimization of the penalized likelihood are displayed in Supplement Fig. 10, and the values for the global parameters are given in Supplement Table 3.

References

Akaike H (1973) Information theory and an extension of the maximum likelihood principle. *International Symposium on Information Theory, 2 nd, Tsahkadsor, Armenian SSR*:267–281.

Cui Y, König J and Keppler D (2001) Vectorial transport by double-transfected cells expressing the human uptake transporter SLC21A8 and the apical export pump ABCC2. *Mol Pharmacol* 60:934–943.

Good I and Gaskins R (1971) Nonparametric roughness penalties for probability densities. *Biometrika* 58:255–277.

Honerkamp J (1994) Analysis of stationary data, in *Stochastic Dynamical Systems* pp 40-89, Wiley-VCH, New York.

Letschert K, Keppler D and König J (2004) Mutations in the SLCO1B3 gene affecting the substrate specificity of the hepatocellular uptake transporter OATP1B3 (OATP8). *Pharmacogenetics* 14:441–52.

Stein WD (1990) Carrier-Mediated Transport: Facilitated Diffusion, in *Channels, Carriers, and Pumps: An Introduction to Membrane Transport* pp 127-171, Academic Press, San Diego.

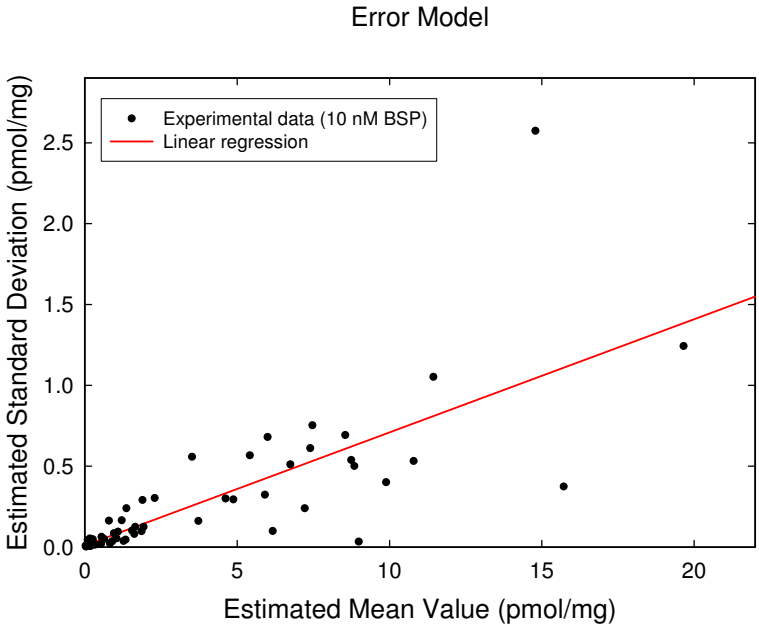

Supplement Figure 8: The estimated standard deviations plotted against the estimated mean values. The statistical fluctuations are large, since the standard deviations were estimated from only three measurements.

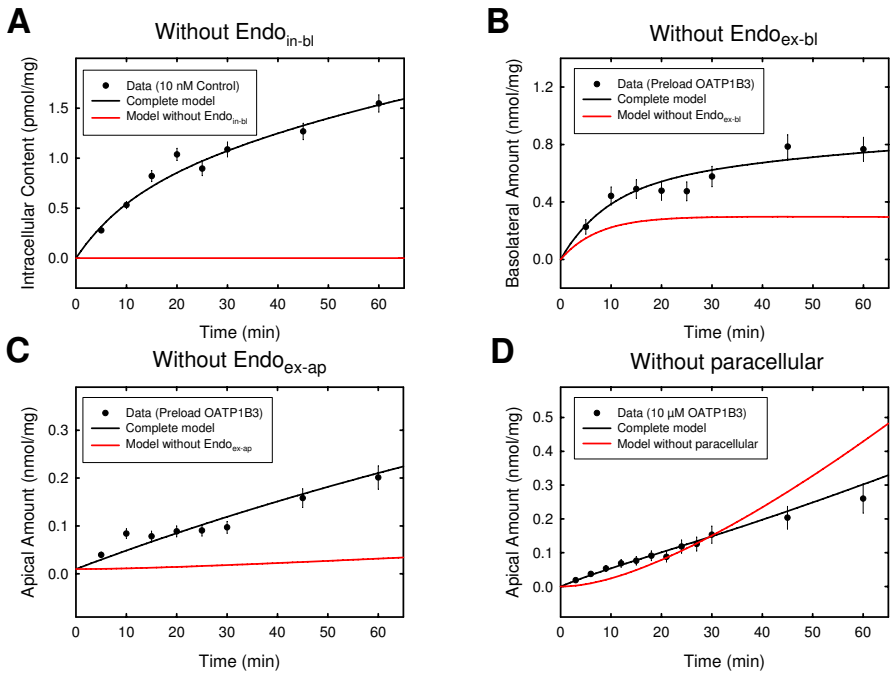

Supplement Figure 9: Comparison of the fits of the smaller models with the fit of the complete model. (*A*) Experiments with 10 nM and 10 μM BSP showed an intracellular accumulation for control cells also. The model lacking the endogenous basolateral uptake transporter cannot explain this accumulation in the control cells. Thus, the model cannot describe the observed data. (*B*) For preloading experiments, the model without the endogeneous basolateral efflux transporter can explain the increase of BSP in the basolateral chamber to only partially. Specifically, it can by the amount that was previously bound non-specifically to the filter membrane during the preloading procedure. For any additional accumulation of BSP in the basolateral chamber, BSP has to be transported back from the intracellular into the basolateral compartment. (*C*) The increase of the apical amount of BSP for the preloading experiments cannot sufficiently be explained by the model lacking the endogenous apical efflux pump. (*D*) When the paracellular transport is missing in the model, the apical amount of BSP at early time points of the experiment is significantly smaller, and at later time points significantly larger than the experimental data. In the beginning, there is no BSP in the intracellular compartment, and thus nothing can be exported into the apical chamber. On the other hand, at later time points, when sufficient amounts of BSP have accumulated in the cells, the apical efflux pump leads to a larger increase of BSP in the apical chamber than experimentally determined.

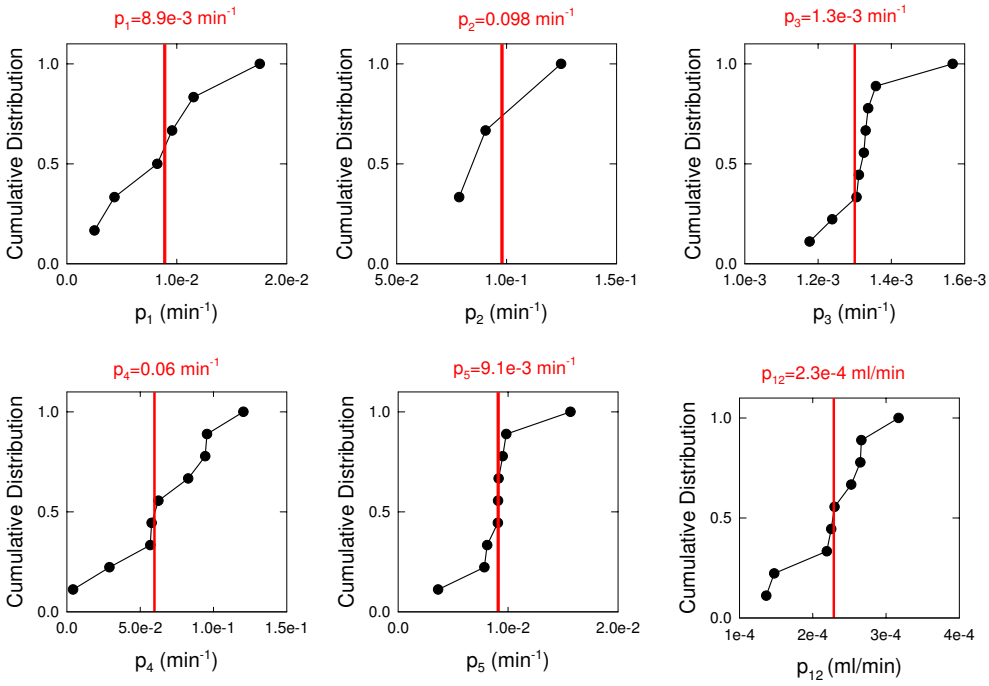

Supplement Figure 10: Cumulative distribution of the local parameters. Each closed circle represents the value of a local parameter in one experiment. Altogether, there were nine experiments: BSP concentrations of 10 μM, 10 nM, and preloading, each for control, single-transfected (OATP1B3) and double-transfected (OATP1B3-ABCC2) cells. For the parameters p_1 and p_2, only six, respectively three values were determined since the control cells do neither express OATP1B3 nor ABCC2, and the single-transfected cells do not express ABCC2.

Supplement Table 2: Akaike Information Criteria (AIC) for each model. The AIC enables the quantitative comparision of different models, favoring the model with the smallest AIC.

	Complete Model	w/o Endo$_{in-bl}$	w/o Endo$_{ex-bl}$	w/o Endo$_{ex-ap}$	w/o paracell.
AIC	-1280	3353	-566	-784	-818

Supplement Table 3: The values of the global parameters and their standard deviations of the resulting fit. Parameters p_8 and p_{10} were fixed since they were not identifiable. The parameters for the volumes V_{bl} and V_{ap} were known from the experimental setup. The basolateral volume V_{bl} was 1.0 ml for the preloading experiments and 1.5 ml for all other experiments.

		mean	std
p_6	$[\frac{mg}{min \cdot nmol}]$	6.4e-5	2.7e-6
p_7	$[min^{-1}]$	0.040	0.002
p_8	$[\frac{nmol}{mg}]$	1000	-
p_9	$[\frac{mg}{min \cdot nmol}]$	0.01	0.01
p_{10}	$[min^{-1}]$	1.6	1.6
p_{11}	$[\frac{nmol}{mg}]$	1000	-
V_{bl}	$[ml]$	1.5/1.0	-
V_{ap}	$[ml]$	1.0	-